



UDC 699.88

SPECTRAL ANALYSIS OF LAMB WAVE PACKETS SCATTERED BY DAMAGE IN LAMINAR COMPOSITES

Pysarenko A.M.

c.ph.-m.s., as.prof.

ORCID: 0000-0001-5938-4107

Odessa State Academy of Civil Engineering and Architecture,
Odessa, Didrihsona, 4, 65029

Abstract. This article presents a novel spectrum decomposition approach for reconstructing the phase velocity dispersion curve of Lamb waves. The method's effectiveness is demonstrated by its ability to recover the dispersion curve over a significantly broader frequency range, covering nearly the entire bandwidth of the incident Lamb wavelet signal. The study highlights that the frequency range of the reconstructed dispersion curve is directly influenced by the bandwidth of the filters used in the decomposition process. It was found that narrower filters lead to superior results, with the narrowest filter achieving a ninety percent coverage of the original signal's bandwidth. However, this improved accuracy comes with the trade-off of increased computational resource requirements and longer processing times due to the larger number of filters needed.

The research includes a presentation of typical B-scan results for the propagation of the A0 Lamb wave mode in laminated composite sample. The dispersion curve data for the relative amplitude were analyzed across three distinct frequency bands. The measurement results, obtained using various filter sets, were compared against the dispersion curve derived from the zero-crossing method for the A0 mode. The presented results, including phase velocity measurements in meters per second, cover a frequency range from zero to five hundred kilohertz, showcasing the method's potential for comprehensive Lamb wave analysis.

Key words: Lamb wave, dispersion curve, filter, signal's bandwidth, laminated composite.

Introduction.

The increasing demand for lightweight, high-performance materials has propelled laminated composites to the forefront of modern engineering. These materials, known for their exceptional specific strength and stiffness, are ubiquitous in critical applications across the aerospace, automotive, and sports industries. However, their inherent layered structure makes them susceptible to a unique class of defects, primarily delaminations and matrix cracks, which can severely compromise their structural integrity [1 - 3]. Unlike surface-level damage, these internal flaws are often difficult to detect using conventional non-destructive testing methods, necessitating the development of more advanced and sensitive techniques. The failure to identify and characterize such damage in its nascent stages can lead to catastrophic failure, highlighting the crucial need for effective and reliable structural health monitoring systems.



Guided wave methods, specifically those utilizing Lamb waves, have emerged as a highly promising solution for the non-destructive evaluation of these plate-like structures [4, 5]. Lamb waves are elastic waves that propagate within the boundaries of a plate, offering the significant advantage of long-range inspection from a single or a small number of excitation points. Their unique characteristics, including multiple propagation modes and frequency-dependent velocities—a phenomenon known as dispersion—make them particularly sensitive to changes in the material properties caused by damage. The interaction of a Lamb wave with an internal inhomogeneity, such as a delamination, causes the wave to scatter. This scattered wave field carries vital information about the nature, size, and location of the defect, which can be extracted through sophisticated signal processing.

The complexity of Lamb wave propagation in laminated composites is a major challenge. These materials are typically anisotropic and heterogeneous, meaning their mechanical properties vary with direction and position. This results in far more complex dispersion curves compared to those of isotropic materials. Furthermore, the presence of defects introduces additional complexity, making the interpretation of wave propagation patterns a non-trivial task. Traditional analysis methods, which often rely on single-frequency or single-mode interrogation, may not be sufficient to provide a comprehensive assessment of the damage, especially for complex or multi-layered defects. Therefore, there is a clear need for advanced analytical frameworks that can effectively handle the intricate complexities of wave scattering in these advanced materials.

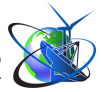
To address the limitations of traditional methods, this research explores the potential of spectral analysis as a powerful tool for a more detailed understanding of damage in composites. Spectral analysis involves decomposing a complex signal into its constituent frequency components. In the context of Lamb waves, this means examining how each frequency within a wave packet interacts with and scatters from a defect. This approach allows for a multi-frequency interrogation of the material, which can provide a richer and more detailed dataset for damage characterization compared to a single-frequency approach. The core idea is that different frequency



components of a Lamb wave are sensitive to different scales and types of damage. Low-frequency components, with their longer wavelengths, are generally more effective at detecting larger, more distributed damage, while higher-frequency components, with shorter wavelengths, are better suited for identifying smaller, more localized defects. By analyzing the entire frequency spectrum of the scattered wave field, we can create a more complete picture of the damage state. This is particularly relevant for laminated composites, where a defect might manifest differently at various scales, such as a small localized delamination that also creates a broader area of matrix degradation.

A key challenge in this spectral approach is the interpretation of the complex scattering patterns. The scattered wave field is not a simple reflection; it is a combination of reflections, transmissions, and mode conversions, all of which are highly dependent on the incident wave frequency and the geometry of the defect. A robust analytical framework is required to process this data and correlate specific spectral features with particular types of damage. This is where the concept of breaking down the dispersion curves comes into play. The research focuses on a novel method that enhances the capabilities of spectral analysis by breaking down the dispersion curves into specific frequency sub-bands. This approach is motivated by the hypothesis that different frequency ranges of the Lamb wave spectrum are preferentially sensitive to different types and scales of damage. By isolating and analyzing these sub-bands, we can effectively filter out extraneous information and highlight the specific spectral signatures associated with particular damage modes. For example, a low-frequency sub-band might be highly sensitive to the overall area of a delamination, as the long wavelengths are influenced by the integrated effect of the defect. Conversely, a high-frequency sub-band might reveal fine details about the crack edges or the presence of smaller micro-cracks surrounding the main defect. By segmenting the analysis in this manner, we can create a multi-scale damage monitoring model. This allows for a more nuanced and accurate characterization of damage that might be missed by an analysis of the full spectrum.

The process involves several key steps. First, a broadband Lamb wave signal is



excited in the composite plate, and the scattered waves are then captured by an array of sensors. Second, the recorded signals are subjected to a spectral decomposition technique, such as the Short-Time Fourier Transform or wavelet analysis, to separate the signal into its frequency components. Third, the phase and group velocities are calculated for each frequency component, and the dispersion curves are reconstructed. Fourth, the reconstructed dispersion curves are then broken down into predefined frequency sub-bands, and the spectral features within each sub-band are analyzed individually to identify and characterize damage. For instance, changes in phase velocity, mode conversion patterns, and amplitude attenuation are examined for each sub-band. Finally, the results from the sub-band analysis are integrated to create a comprehensive damage model. This model correlates the specific spectral signatures in each sub-band with the physical characteristics of the damage. This method offers a significant advantage by allowing for the separation of damage-related effects from the intrinsic material properties. For example, by analyzing a specific sub-band that is known to be particularly sensitive to delamination, we can create a damage metric that is less influenced by variations in the material's elastic properties in other frequency ranges. This targeted analysis can lead to higher detection sensitivity and reduced false positives. The overall objective of this research is to create a robust and reliable damage monitoring model for laminated composites. This will be achieved by leveraging a detailed spectral analysis of Lamb wave scattering from inhomogeneities, with a specific focus on the results obtained by breaking down the dispersion curves into distinct frequency sub-bands. The ultimate goal of this study is to develop a more accurate and sensitive method for the early detection and comprehensive characterization of damage in these critically important materials, thereby enhancing the safety and longevity of structures that rely on them.

Bandpass filtering of signals

The calculation model used in this study assumed the presence of multiple heterogeneities randomly distributed in each layer of the laminated composite. The number of composite layers was fixed. Deformation detection was performed based on the analysis of the kinetic characteristics of Lamb wave packets dispersed at local



deformations of each composite layer. At each stage of calculations, both the signal frequency and the phase velocity of the Lamb wave were determined. The resulting set of phase velocities and frequencies formed a set of dispersion curves, the non-stationary nature of which characterized the unique distribution of heterogeneities along each layer.

The zero-crossing algorithm assumes the possibility of decomposing the measured signals $u_i(t)$ at different distances into a set of signals with a limited bandwidth $u_{ik}(t)$. Such a procedure becomes possible provided that the signals $u_i(t)$ are filtered using bandpass filters with a narrower bandwidth than the bandwidth of the incident spectrum.

At the next step for each filtered signal $u_{ik}(t)$ the delay times t_{imk} and $t_{(i+1)mk}$ are estimated. In this way, the phase velocities c_{pmk} and frequencies f_{mk} are calculated. Then, the obtained sets (f_{mk}, c_{pmk}) can be represented as segments of the phase velocity dispersion curve.

Each section of the dispersion curve obtained using one of the filters can be reconstructed in a relatively narrow passband. In addition, scanning the filter's central frequency in wide frequency ranges will allow covering a large part of the falling spectrum.

The frequency spectrum of two adjacent signals can be represented as

$$U_i(f) = FT[u_i(t)]. \quad (1)$$

$$U_{i+1}(f) = FT[u_{i+1}(t)], \quad (2)$$

where

$u_i(t)$ is the signal measured at distance $x_i(t)$;

$u_{i+1}(t)$ is the signal measured at distance $x_{i+1}(t)$;

FT is the Fourier transform.

Adjacent bands of the frequency spectra are filtered by k Gaussian bandpass filters with predetermined parameters

$$U_{ik}(f) = U_i(f) \cdot B_k(f). \quad (3)$$

$$U_{(i+1)k}(f) = U_{i+1}(f) \cdot B_k(f). \quad (4)$$



where the frequency response of k -th bandpass filter is

$$B_k(f) = \exp\left\{4\ln(0.5) \cdot \Delta B^{-2} \cdot [f - f_L - (k-1)df]^2\right\}, \quad k=1,2,\dots,K. \quad (5)$$

where

f_L is the left frequency filter edge;

f_H is the central part of frequency filter edge;

ΔB is the filter bandwidth;

the frequency domain df is

$$df = \frac{f_H - f_L}{K-1}. \quad (6)$$

The signal reconstruction using the Fourier transform has the following form

$$u_{ik}(t) = FT^{-1}[U_{ik}(f)]. \quad (7)$$

$$u_{(i+1)k}(t) = FT^{-1}[U_{(i+1)k}(f)]. \quad (8)$$

At the next stage of the numerical method, the phase velocity can be estimated according to the following relation

$$c_{pmk} = \frac{x_{i+1} - x_i}{t_{(i+1)mk} - t_{imk}}. \quad (9)$$

Using the data on the duration of the half-periods of the first signal, it is possible to estimate the equivalent frequencies to which the calculated values of the phase velocity should be assigned

$$f_{imk} = \frac{0.5}{t_{i(m+1)k} - t_{imk}}. \quad (10)$$

Comparison of the results obtained using the proposed hybrid method and the previous version of the reference zero-crossing method showed that the zero-crossing method recovers the phase velocity dispersion curve in the frequency range of 286 – 319 kHz. This bandwidth is only 8% of the original signal bandwidth.

Meanwhile, the proposed spectrum decomposition approach allows us to recover the phase velocity dispersion curve in a significantly wider frequency range. This range covers almost the entire bandwidth of the incident Lamb wavelet signal. It should be



noted that the frequency ranges in which the dispersion curve is reconstructed depend significantly on the bandwidth of the filters used in the spectrum decomposition approach.

For example, for the 120 kHz filter, 70% coverage of the incident signal bandwidth was achieved. Finally, the best results were achieved with the narrowest filter (40 kHz bandwidth). For this narrowed filter, the reconstructed dispersion curve covers 90% of the original bandwidth.

In summary, it can be argued that narrow filters are more efficient, but this leads to a large number of filters, which generates more computational resources and longer processing times.

Table 1 - Dispersion dependences for A0 mode of the Lamb wave

A-band		B-band		C-band	
f , kHz	A'	F , kHz	A'	F , kHz	A'
15.9304	0.0152	157.2193	0.5169	304.7936	0.5203
25.3012	0.0338	158.1551	0.4882	311.3182	0.5458
34.6720	0.1083	162.8342	0.5017	318.7750	0.5085
41.2316	0.2183	170.3209	0.4595	322.5033	0.5864
47.7912	0.2470	176.8717	0.5456	328.0959	0.6661
58.0991	0.2369	185.2941	0.5253	327.1638	0.7322
62.7845	0.3063	187.1658	0.6284	333.6884	0.6898
61.8474	0.4856	195.5882	0.7128	341.1451	0.7254
69.3440	0.6125	199.3316	0.7010	343.9414	0.6644
74.0295	0.4399	199.3316	0.7517	347.6698	0.5458
78.7149	0.3012	203.0749	0.7973	356.9907	0.5746
85.2744	0.4467	209.6257	0.7720	361.6511	0.6085
87.1486	0.5330	213.3690	0.7483	364.4474	0.5339
89.9598	0.6261	213.3690	0.8142	363.5153	0.4864
96.5194	0.5753	217.1123	0.8953	362.5832	0.3814
104.0161	0.7547	218.9840	0.9865	366.3116	0.2712
111.5127	0.5381	233.0214	0.8666	377.4967	0.1780
113.3869	0.6819	237.7005	0.6791	387.7497	0.1051
115.2610	0.7902	246.1230	0.7500	399.8668	0.1322
122.7577	0.9306	248.9305	0.8497	411.9840	0.1797
126.5060	0.8190	254.5455	0.9662	424.1012	0.1102
136.8139	0.7580	263.9037	0.9578	430.6258	0.0678
143.3735	0.7733	266.7112	0.8868	441.8109	0.1186



Typical B-scan results for the propagation of the A0 Lamb wave mode in a 2 mm thick laminated composite sample are presented in Table 1. The dispersion curve data for the relative amplitude are divided into three ranges: A-band (0 - 150 kHz). B-band (150-300 kHz) and C-band (300-500 kHz).

The measurement results using different sets of the filters (where P is the number of filters) are obtained and compared with the dispersion curve of zero-crossing method (ZCM) for A0 mode of the Lamb wave ($f \in 0 \div 500$ kHz). The results for phase velocity c_p (measured in m/s) are presented in Table 2.

Table 2 - Dispersion curves for different methods

$P = 4$		$P = 12$		ZCM	
f, kHz	$c_p, \text{m/s}$	f, kHz	$c_p, \text{m/s}$	f, kHz	$c_p, \text{m/s}$
76.923	1207.41	59.64	1047.13	65.22	1047.20
88.942	1304.38	78.31	1183.57	76.09	1114.29
102.163	1393.27	104.22	1332.40	88.77	1186.34
123.798	1522.56	123.49	1429.15	99.03	1258.39
142.428	1608.75	135.54	1483.72	109.90	1340.37
156.851	1654.55	149.40	1548.22	122.58	1370.19
164.063	1724.58	175.30	1652.40	140.10	1459.63
177.885	1746.13	204.82	1759.07	152.78	1504.35
183.894	1805.39	224.10	1791.32	174.52	1603.73
197.716	1837.71	246.39	1890.54	191.43	1638.51
212.740	1905.05	268.67	1930.23	210.14	1740.37
228.966	1937.37	295.18	1997.21	230.68	1780.12
234.375	1983.16	310.84	2017.05	254.23	1852.17
253.005	2020.88	322.89	2051.78	269.93	1899.38
265.625	2090.91	339.76	2074.11	289.25	1926.71
284.856	2115.15	355.42	2126.20	300.12	1968.94
302.885	2150.17	384.94	2163.41	322.46	1996.27
316.707	2198.65	396.39	2190.70	346.01	2055.90
332.933	2195.96	413.25	2203.10	375.00	2088.20
345.553	2263.30	419.28	2230.39	402.17	2147.83
362.380	2268.69	431.33	2230.39	423.31	2165.22
385.216	2325.25	439.76	2250.23	434.18	2190.06
405.649	2338.72	450.60	2255.19	445.05	2197.52
426.082	2389.90	463.25	2292.40	469.20	2222.36
449.519	2419.53	481.33	2299.84	486.11	2249.69

The dispersion curves for $P = 4$, $P = 12$ and ZCM are practically indistinguishable



in the range of 60 - 100 kHz. The maximum difference in the phase velocities of Lamb wave packet propagation is observed for the sub-range of 400 - 480 kHz. Two more features of these dispersion curves should be noted. First, the relative difference in the phase velocities for $P = 12$ and ZCM is significantly smaller compared to the difference for $P = 12$ and $P = 4$. In addition, all three dispersion curves have a similar functional nature, characterized by insignificant nonlinearity. The numerical values of the phase velocities increase approximately by a factor of 1.15 for the specified integral frequency range.

Summary and conclusions.

This study introduces a novel spectrum decomposition approach for recovering the phase velocity dispersion curve of Lamb waves. A key finding is that this method significantly broadens the frequency range over which the dispersion curve can be reconstructed, encompassing nearly the entire bandwidth of the incident Lamb wavelet signal. The effectiveness of the approach is directly tied to the bandwidth of the filters employed. It was observed that narrower filters yield superior results in terms of frequency coverage. Specifically, the narrowest filter tested, with a bandwidth of forty kilohertz, allowed for the reconstruction of the dispersion curve across ninety percent of the original signal's bandwidth. However, this increased accuracy comes at a cost, as using narrower filters necessitates a greater number of filters, leading to higher computational demands and extended processing times.

The research also presents typical B-scan results for the propagation of the A0 Lamb wave mode in a two-millimeter-thick laminated composite sample. The dispersion curve data for relative amplitude were analyzed across three distinct frequency bands. The measurement results, obtained using various sets of filters, were compared against data from the zero-crossing method for the A0 mode. The phase velocity measurements, in meters per second, were presented across a frequency range from zero to five hundred kilohertz. The proposed method demonstrates its capability to provide comprehensive dispersion curve data, offering a valuable alternative to traditional techniques.

**References:**

1. Barry, T. J., Kesharaju, M., Nagarajah, C. R., & Palanisamy, S. (2016). Defect characterisation in laminar composite structures using ultrasonic techniques and artificial neural networks. *Journal of Composite Materials*, issue 50, vol. 7, pp. 861-871
DOI: 10.1177/0021998315584651
2. Iarve, E. V., Gurvich, M. R., Mollenhauer, D. H., Rose, C. A., & Dávila, C. G. (2011). Mesh-independent matrix cracking and delamination modeling in laminated composites. *International journal for numerical methods in engineering*, issue 88, vol. 8, pp. 749-773
DOI: 10.1002/nme.3195
3. Alfano, G., & Crisfield, M. (2001). Finite element interface models for the delamination analysis of laminated composites: mechanical and computational issues. *International journal for numerical methods in engineering*, issue 50, vol. 7, pp. 1701-1736
DOI: 10.1002/nme.93
4. Ricci, F., Monaco, E., Maio, L., Boffa, N. D., & Mal, A. K. (2016). Guided waves in a stiffened composite laminate with a delamination. *Structural Health Monitoring*, issue 15, vol. 3, pp. 351-358.
DOI: 10.1177/1475921716636335
5. Philibert, M., Yao, K., Gresil, M., & Soutis, C. (2022). Lamb waves-based technologies for structural health monitoring of composite structures for aircraft applications. *European Journal of Materials*, issue 2, vol. 1, pp. 436-474
DOI: 10.1080/26889277.2022.2094839

Article sent: 10.08.2025

© Pysarenko A.M.